Development and evaluation of a driver circuitry for miniature spectrometers used in cold environments

Nan, Liwen; Wang, Hangzhou; Han, Jiwan; Huang, Hui; Song, Hong; Chen, Ying

Published in:
IEICE Electronics Express

DOI:
10.1587/elex.14.20170876

Publication date:
2017

Citation for published version (APA):
Nan, L., Wang, H., Han, J., Huang, H., Song, H., & Chen, Y. (2017). Development and evaluation of a driver circuitry for miniature spectrometers used in cold environments. *IEICE Electronics Express*, *14*(20), [20170876]. https://doi.org/10.1587/elex.14.20170876

ELectronics EXpress

LETTER

IEICE Electronics Express, Vol.14, No.20, 1–12

Development and evaluation of a driver circuitry for miniature spectrometers used in cold environments

Liwen Nan[1], Hangzhou Wang[1a)], Jiwan Han[2], Hui Huang[1], Hong Song[2], and Ying Chen[1]

[1] *Ocean College, Zhejiang University, Zhoushan 316021, China*

[2] *Institute of Biological, Environmental & Rural Sciences, Aberystwyth University, SY23 3EE, UK*

a) *hangzhouwang@zju.edu.cn*

Abstract: Special attention should be paid during the development of the driver circuitries for miniature spectrometers when using them in extreme environments, especially when the ambient temperature changes tremendously. In this study, a driver circuitry for a miniature spectrometer is developed by providing a basic control signal and ADC circuitry. Meanwhile, temperature stability and power consumption are considered. The performance of the driver circuitry is evaluated comprehensively from −50°C to 30°C. The lower boundary is below the operating range of most electronic parts adopted. Based on these examinations, temperature dependence, linearity and conversion accuracy of the ADC circuitry are quantified. And a correction algorithm is developed to correct any deviation in the driver circuitry with an uncertainty of around ±20 Counts. The practicality of the driver circuitry is also identified. This approach provides a general framework for developing driver circuitry for miniature spectrometers which will face tremendous variations in the ambient temperature.

Keywords: design, evaluation, driver circuitry, miniature spectrometer, temperature

Classification: Circuits and modules for electronic instrumentation

References

[1] M. C. Serreze, *et al.*: "Perspectives on the Arctic's shrinking sea-ice cover," Science **315** (2007) 1533 (DOI: 10.1126/science.1139426).

[2] J. C. Comiso, *et al.*: "Accelerated decline in the Arctic sea ice cover," Geophys. Res. Lett. **35** (2008) (DOI: 10.1029/2007GL031972).

[3] J. C. Comiso: "Large decadal decline of the Arctic multiyear ice cover," J. Clim. **25** (2012) 1176 (DOI: 10.1175/JCLI-D-11-00113.1).

[4] D. K. Perovich, *et al.*: "Increasing solar heating of the Arctic Ocean and adjacent seas, 1979–2005: Attribution and role in the ice-albedo feedback," Geophys. Res. Lett. **34** (2007) L19505 (DOI: 10.1029/2007GL031480).

[5] J. C. Stroeve, *et al.*: "The Arctic's rapidly shrinking sea ice cover: a research synthesis," Clim. Change **110** (2012) 1005 (DOI: 10.1007/s10584-011-0101-1).

DOI: 10.1587/elex.14.20170876
Received August 23, 2017
Accepted September 11, 2017
Publicized September 28, 2017
Copyedited October 25, 2017

[6] D. Perovich, *et al.*: "Solar partitioning in a changing Arctic sea-ice cover," Ann. Glaciol. **52** (2011) 192 (DOI: 10.3189/172756411795931543).
[7] M. Nicolaus, *et al.*: "Seasonality of spectral albedo and transmittance as observed in the Arctic Transpolar Drift in 2007," J. Geophys. Res. **115** (2010) C11011 (DOI: 10.1029/2009JC006074).
[8] M. Nicolaus, *et al.*: "A modern concept for autonomous and continuous measurements of spectral albedo and transmittance of sea ice," Cold Reg. Sci. Technol. **62** (2010) 14 (DOI: 10.1016/j.coldregions.2010.03.001).
[9] H. Wang, *et al.*: "A fiber optic spectrometry system for measuring irradiance distributions in sea ice environments," J. Atmos. Ocean. Technol. **31** (2014) 2844 (DOI: 10.1175/JTECH-D-14-00108.1).
[10] Ocean Optics, Inc.: USB2000+ Fiber Optic Spectrometer (2016) http://oceanoptics.com/wp-content/uploads/USB2000-Operating-Instructions1.pdf.
[11] K. K. Hamamatsu: mini-spectrometer with USB1.1 (2016) http://www.hamamatsu.com/resources/pdf/ssd/c10082md_etc_kacc1119e.pdf.

1 Introduction

Sea ice in the Arctic is becoming less, thinner and younger in recent several decades, which brings significant influence to the global climate change, marine ecosystem, global shipping, et al. [1, 2, 3] It denotes that these variations are primarily determined by two factors, thermodynamic and dynamic process in the Arctic and the solar radiation which is one of the most important factors [4, 5, 6]. Solar radiation not only contributes to the melting of sea ice but also helps to shape the species and biomass of the marine plankton in the Arctic. Therefore, great efforts have been made to measure solar radiation distribution above or below the Arctic sea ice [7, 8]. A fiber optic spectrometry system is proposed to measure spectral intensity of solar radiation at different depths of sea ice, autonomously and year-roundly [9]. The proposed system adopts one photodiode array miniature spectrometer to detect solar radiation signals collected from multiple fiber probes located at different depths of the sea ice. However, to our knowledge, field application of this kind of miniature spectrometer in the Arctic has not been reported previously, neither does its driver circuitry. The driver circuitries of most commercial spectrometers are not applicable for our application since they are operated via a USB interface with relatively complicated driver software which will increase system complexity and the chance of system malfunction [10, 11]. On top of this, the lower limit of the operating temperature range of these driver circuitries is far higher than that of our system.

A driver circuitry is developed for this miniature spectrometer by providing a basic control signal and ADC circuitry while overcoming the extremely cold ambient temperature. The temperature in the Arctic winter could readily reach −40°C and the proposed operating temperature of the spectrometry system even could reach as low as −50°C. This extremely low temperature is below the lowest operating temperature of most electrical parts and devices and brings great challenges to the driver circuitry. Therefore, the temperature is the primary concern during the development of the driver circuitry. Furthermore, the performance of the driver circuit is assessed comprehensively from −50°C to 30°C, and a correction

DOI: 10.1587/elex.14.20170876
Received August 23, 2017
Accepted September 11, 2017
Publicized September 28, 2017
Copyedited October 25, 2017

algorithm is developed to correct any deviation of the driver circuitry on the basis of the assessments. The performance of the spectrometer together with the driver circuitry is also examined, to verify the practicability of the driver circuitry.

2 Spectrometer and driver circuitry considerations

The miniature spectrometer adopted in the spectrometry system is a compact module (C11009MA, Hamamatsu Photonics K. K., Japan) with a spectral range of 340~780 nm covering the range we are interested in (e.g., 400~700 nm). Apart from the external electrical interface, all of other optical components and electronics are sealed inside a metal shell which protects the spectrometer from the influence of condensation of the airborne water vapor when the ambient temperature drops below the dew point (Fig. 1). Simply provided with timing signals (e.g., ST and CLK), the spectrometer can output the photoelectrically converted voltages corresponding to its 256-pixel photodiodes one-by-one via a common Video line (Fig. 1 and Table I). Therefore, the timing signals generation function should be involved in the driver circuitry to make the spectrometer work properly. And a low-noise analog to digital converter (ADC) circuitry should be also involved for accurately digitizing the analog voltage signals, to facilitate the subsequent data storage and analysis. Additionally, system complexity and power consumption are also considered, in view of the autonomous and year-round application in the extremely cold sea ice environment.

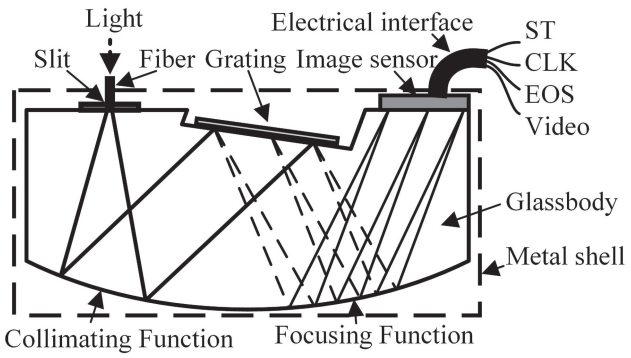

Fig. 1. Schematic diagram of the miniature spectrometer used in this study

Table I. Terminal name and general description of the electrical interface of the spectrometer.

Terminal name	Description	Direction
ST	Sensor scan start signal	Input
CLK	Sensor scan synchronization signal	Input
Video	Sensor video signal output	Output
EOS	Sensor end of scan signal	Output

DOI: 10.1587/elex.14.20170876
Received August 23, 2017
Accepted September 11, 2017
Publicized September 28, 2017
Copyedited October 25, 2017

3 Design of the driver circuitry

As mentioned above, the timing signals generation and ADC are the most important parts of the driver circuitry. In this study, the former (e.g., generation of ST and CLK) was separately generated by two general-purpose I/O (GPIO) ports of a microcontroller, the latter was based on a 16-bit low-power ADC chip, and the cooperation of entire driver circuitry was handled by the microcontroller (Fig. 2). The low-power microcontroller (ATxmega128A1U, Atmel Corporation, USA) has 128 KB flash memory and 8 KB SRAM which are very important for temporary storage of the spectrometry measurements before they are stored in an SD card. To keep the consistency and minimize temperature dependence of integration time (e.g., t_{int} in Fig. 3a) applied to the spectrometer over the entire 80°C range of operating temperatures, a temperature compensated crystal oscillator (TCXO) with a frequency stability of ±0.3 ppm (parts per million) over −40°~85°C was adopted to function as the system clock source of the microcontroller. And the period of t_{int} was controlled by an internal 16-bit timer working at interrupt mode. The TCXO has a frequency of 12.8 MHz, to facilitate the fast readout of the spectrometry measurement. Since the maximum output (e.g., offset voltage and saturation output) of the spectrometer specified by the vendor is ~4.0 V, the reference voltage of the ADC chip (AD7988-5, Analog Devices Inc., USA) was provided by a 5 V ultra low noise voltage reference chip with an initial accuracy of ±2 mV, to ensure all the spectrometry measurement fall into the input range of the ADC circuitry. The adoption of the low noise ADC chip and ultra low noise voltage reference chip is also critical to minimize the noise generated by the ADC circuitry which might be coupled to the spectrometry measurement during the digitizing process ultimately.

3.1 Timing coordination of the spectrometer and ADC

The timing chart of the spectrometer is shown in Fig. 3a. The spectrometer starts a new scan from the rising edges of the ST signal. At each rising edge of the CLK signal, the charge accumulated in each pixel photodiode of the spectrometer is

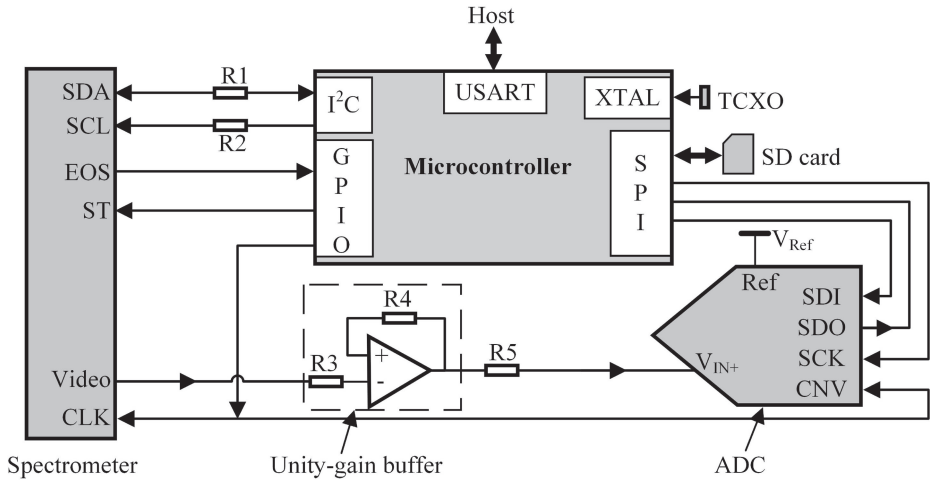

Fig. 2. Schematic of the driver circuitry of the spectrometer. The arrows represent data flow of the spectrometer and the driver circuitry.

DOI: 10.1587/elex.14.20170876
Received August 23, 2017
Accepted September 11, 2017
Publicized September 28, 2017
Copyedited October 25, 2017

converted into a voltage signal by a common internal charge amplifier and then outputted via a common Video line in turn. It should be noticed that, even though integration time for each pixel photodiode is the same, the scan timing differs from pixel to pixel. Therefore, the frequency of the CLK signal should be as fast as possible to minimize the influence of the potential intensity fluctuation of the incident light during field application.

The timing chart of the ADC chip is shown in Fig. 3b. The ADC chip starts the conversion process at each rising edge of the CNV (e.g., convert input) signal, and starts the acquisition process at each falling edge of the CNV. During the acquisition process, the converted result is outputted to the microcontroller via an SPI interface (e.g., SCK and SDO) with MSB (Most Significant Bit) delivered first. To synchronize timing the spectrometer and the ADC, both CLK and CNV are provided by a common GPIO pin of the microcontroller (Figs. 2 and 3).

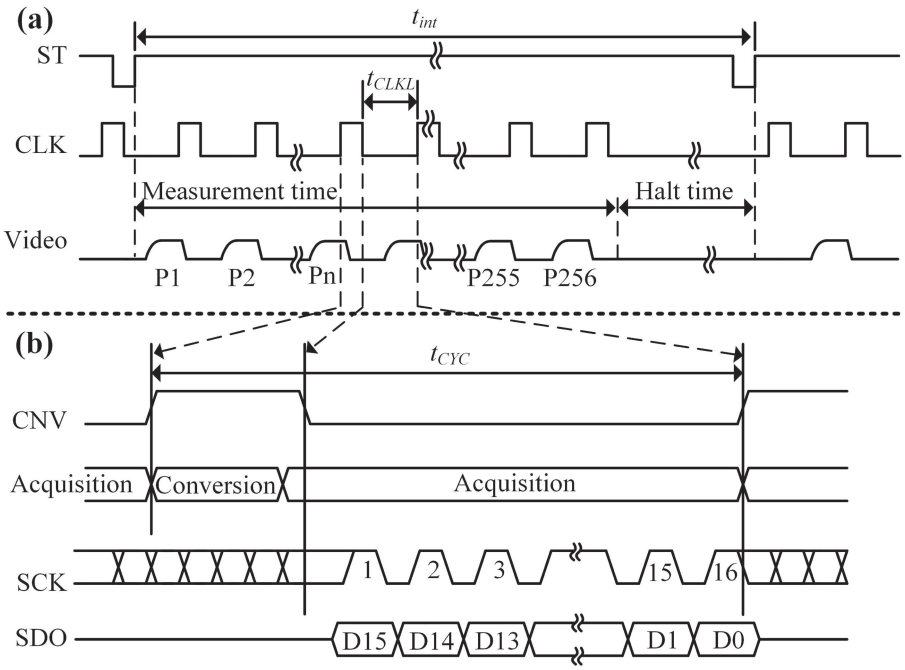

Fig. 3. The timing chart of (a) the spectrometer and (b) the ADC.

3.2 Speed coordination of the spectrometer and ADC

Apart from the timing synchronization of the spectrometer and the ADC, the speed of them should be matched as well to make sure the analog measurement outputted from the spectrometer could be accurately digitized by the ADC. The minimum readout width of the CLK signal (t_{CLKL} in Fig. 3a) of the spectrometer specified by the vendor is 1 µs, therefore maximum readout frequency for each pixel photodiode should be lower than 1 MHz. While the minimum time interval between conversions (t_{CYC} in Fig. 3b) of the ADC chip is 2 µs, which determines that the maximum working speed f_{max} of the combination of the spectrometer and the driver circuitry is 0.5 MHz. This speed could be readily satisfied by the 12.8 MHz TCXO. Therefore, the minimum integration time min(t_{int}) of the system is calculated by

DOI: 10.1587/elex.14.20170876
Received August 23, 2017
Accepted September 11, 2017
Publicized September 28, 2017
Copyedited October 25, 2017

$$\min(i_{int}) = \frac{1}{f_{max}}(\text{number of pixels} + 2) = 2 \times 258 = 516\,\mu\text{s} \quad (1)$$

However, in view that the incident light level is not very strong in the field application, the actual minimum integration time adopted by the system is 1 ms to facilitate the subsequent data analysis and processing.

3.3 Auxiliary design

In addition to the timing signal generation and ADC circuitry, there are still other auxiliary considerations during the design of the driver circuitry. A digital thermosensor was embedded inside the spectrometer which was used to indicate actual temperature of the spectrometer. The working of the thermosensor and the readout of the measured temperature were controlled by the microcontroller via an I^2C interface (e.g., SDA and SCL in Fig. 2). A serial communication interface (USART) was also included in this circuitry to facilitate the debugging and data communication. In order to minimize the noise of the driver circuitry, the digital ground was isolated from analog ground using magnetic beads, besides the adoption of the low-noise chips and parts stated above. To decrease the power consumption of the entire system, the microcontroller would enter sleep mode after it powered off the ADC circuitry and spectrometer during the non-working time.

4 Performance evaluation of the driver circuitry

Because the data regarding the temperature characteristics of this ADC circuitry are largely unavailable for the range of temperatures we specify for operation (−50°~30°C), the potential temperature dependence of the ADC circuitry is assessed. Meanwhile, linearity and conversion accuracy of the ADC circuitry is also examined. Careful evaluation of these performances is essential to estimate the degree how the spectrometry measurement been undistorted digitized and to facilitate the development of the subsequent correction algorithm.

4.1 Experimental setup

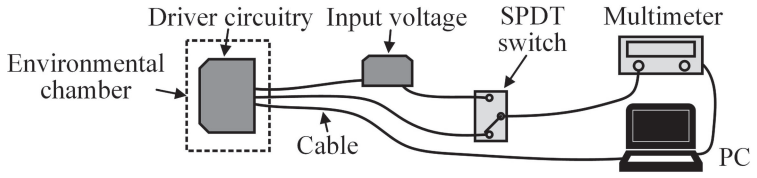

Fig. 4. Test configuration of the driver circuitry used to assess its temperature dependence.

As shown in Fig. 4, we put the driver circuitry inside an environmental test chamber and measured the ADC output over a range of −50°~30°C, while providing with an adjustable input voltage. The input voltage generated by a nominal 5 V voltage reference chip and a potentiometer ranged from 0.2 V to 4.2 V for this examination, which should cover the entire output range of the spectrometer since the maximum output was ~4.0 V and the minimum output (e.g.,

DOI: 10.1587/elex.14.20170876
Received August 23, 2017
Accepted September 11, 2017
Publicized September 28, 2017
Copyedited October 25, 2017

offset voltage) was ~1.0 V. The measurements were taken every 5°C. At each test temperature, we measured 256 times for each input voltage to minimize the statistical uncertainty. Meanwhile, the input voltage and the reference voltage of the ADC circuitry were measured by a common 6.5 bits high-precision multimeter, and the switching of each channel was controlled by a single pole double throw (SPDT) switch.

4.2 Temperature dependence of the ADC circuitry

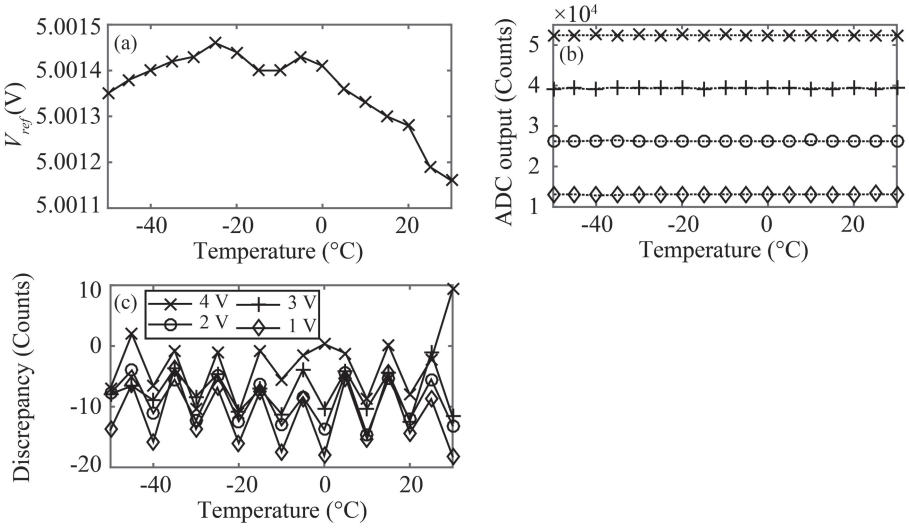

Fig. 5. Temperature dependence of (a) the reference voltage, (b) the ADC output at four input voltages, and (c) discrepancy of the measured ADC output at the same four input voltages as (b). The dashed lines in (b) are the ideal output of the ADC circuitry.

The results indicate that temperature dependence of the reference voltage is roughly in a parabolic manner, with the maximum value of 5.00146 V at −25°C and a minimum value of 5.00116 V at 30°C (Fig. 5a). This corresponds to a variation of at most 0.006% over the entire 80°C range of temperatures. In order to analyze temperature dependence of the ADC output, we averaged the measurements at each input voltage over the times collected. The results denote that the measured ADC output is extremely stable from −50°C to 30°C under each of the test input voltage (Fig. 5b). And it is very close to the ideal output of the ADC circuitry C_{ideal} at each input voltage V_{in}, which is given by (the dashed lines in Fig. 5b)

$$C_{ideal}(V_{in}, T) = \frac{V_{in}}{V_{ref}(T)} \times 2^{16} = \frac{2^{16}}{V_{ref}(T)} V_{in} \tag{2}$$

where V_{ref} is the reference voltage, and T is the temperature. The discrepancy between the measured ADC output and C_{ideal} is all within ±20 Counts from −50°C to 30°C (Fig. 5c). Hence, it could be found that the temperature stability of the ADC circuitry is excellent, which is critical for reducing temperature-induced biases in the entire system (e.g., driver circuitry and the spectrometer) due to the unavoidable temperature variation in the Arctic.

DOI: 10.1587/elex.14.20170876
Received August 23, 2017
Accepted September 11, 2017
Publicized September 28, 2017
Copyedited October 25, 2017

4.3 Linearity and conversion accuracy of the ADC circuitry

As mentioned in the previous sections, the output of the spectrometer will be digitized by the ADC circuitry. In order to simplify the correction process and enhance the conversion accuracy, it is ideal that all of the analog spectrometer output could be proportionally converted into counts by the ADC circuitry following Eq. (2).

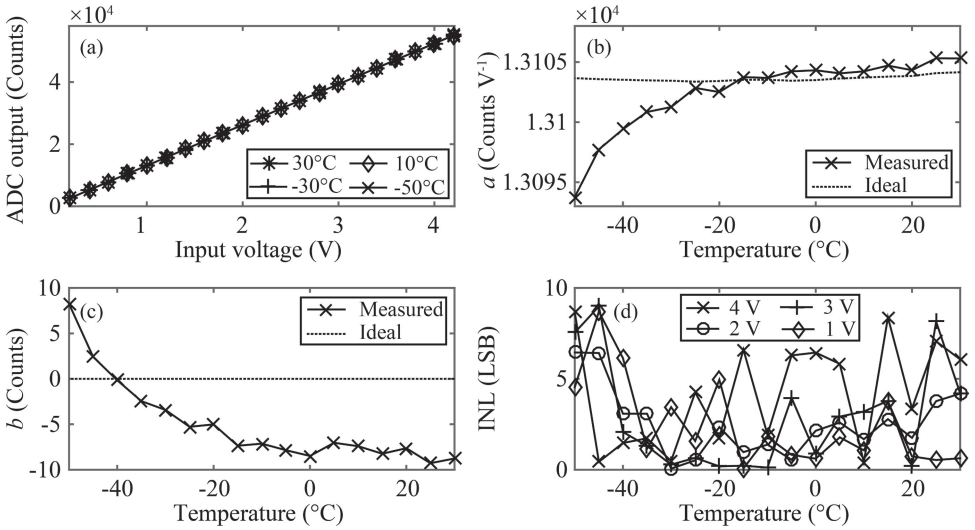

Fig. 6. (a) Input-output relationship of the ADC circuitry at four temperatures; temperature dependence of (b) the fitted slope, (c) the fitted intercept, and (d) INL of the ADC circuitry.

From the above assessments, we observe that the ADC output increase strongly proportionally with higher input voltage with R^2 bigger than 0.9999 and this relationship differ slightly, for each test temperature (Fig. 6a). It verifies that linearity of the ADC circuitry is excellent for the entire range of input voltages (e.g., 1∼4 V) and operating temperatures (e.g., −50°∼30°C) we concerned. Therefore, a linear model is adopted to approximate the ADC output C_{fit} as a function of V_{in} by

$$C_{fit}(V_{in}, T) = a(T)V_{in} + b(T) \tag{3}$$

Where a and b are the least squares fitted slope and intercept, respectively. In general, a differs slightly from the slope of Eq. (2) (e.g., $2^{16}V_{ref}{}^{-1}(T)$) over −50°∼30°C (Fig. 6b). a increases roughly parabolically with warmer temperature from smaller than 9.9 Count V^{-1} at −50°C to bigger than 0.2 Count V^{-1} at −10°C. Above −10°C, a is almost stable at 0.9 Count V^{-1} bigger than the slope of Eq. (2). In contrast, b is decreased roughly parabolically with warmer temperature from 8.2 Counts at −50°C to −8.8 Counts at 30°C (Fig. 6c). The integral nonlinearity (INL) of the ADC circuitry is smaller than 10 LSB over the entire 80°C range of operating temperatures, which is acceptable for our application (Fig. 6d).

5 Correction algorithm for the ADC circuitry

Based on the above assessments, we find that the measured ADC output differs from the ideal ADC output very slightly for each input voltage from −50°∼30°C

DOI: 10.1587/elex.14.20170876
Received August 23, 2017
Accepted September 11, 2017
Publicized September 28, 2017
Copyedited October 25, 2017

(Figs. 5b and 5c). However, a correction algorithm is still developed to minimize the deviation in the ADC circuitry as much as possible. The degree that the measured ADC output deviating from the ideal one could be approximated by the ratio of them α by

$$\alpha(T) = \frac{C_{ideal}(V_{in}, T)}{C_{fit}(V_{in}, T)} = \frac{2^{16} V_{ref}^{-1}(T) V_{in}}{a(T) V_{in} + b(T)} = \frac{2^{16} V_{ref}^{-1}(T)}{a(T)} \frac{V_{in}}{V_{in} + a^{-1}(T) b(T)} \quad (4)$$

Since a is at least three orders of magnitude greater than b at each temperature T and V_{in} is all bigger than 1 V for our application, Eq. (4) could be simplified as

$$\alpha(T) = \frac{2^{16} V_{ref}^{-1}(T)}{a(T)} \quad (5)$$

We observe that α decreases roughly linearly with warmer temperature from 1.00041 at −50°C to 0.99981 at 30°C (Fig. 7a). Assuming that the relationship between the ideal ADC output and the counts as measured by this ADC circuitry remains constant over the input voltages other than those we adopted and the temperatures other than we measured in this study, the bias of this ADC circuitry could be corrected by

$$C_{corr}(V_{in}, T) = \alpha(T) C_{meas}(V_{in}, T) \quad (6)$$

where C_{corr} and C_{meas} are the corrected and directly measured ADC output respectively. The value of the correction coefficient α at the temperatures other than we measured could be predicted using a linear interpolation by

$$\alpha(T) = \alpha(T_i) + [\alpha(T_{i+1}) - \alpha(T_i)] \frac{T - T_i}{T_{i+1} - T_i} \quad (7)$$

Where T_i and T_{i+1} are the test temperatures we adopted, $T_i \leq T < T_{i+1}$, and $1 \leq i \leq 16$.

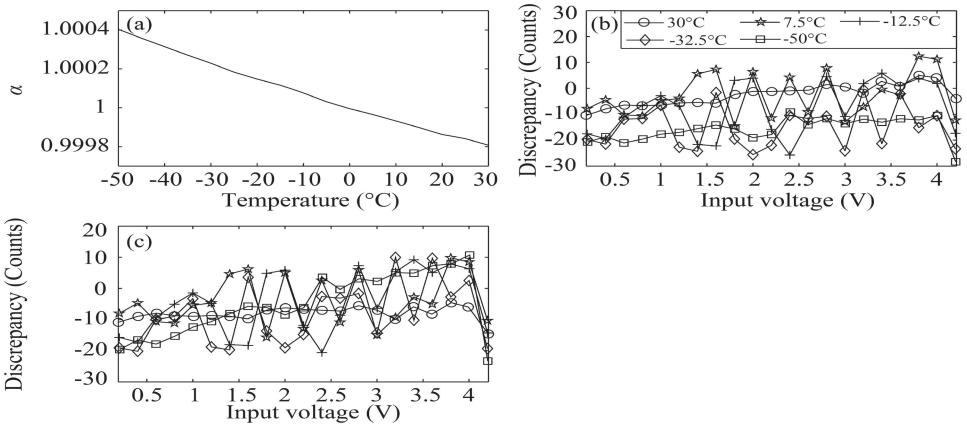

Fig. 7. (a) Temperature dependence of the correction coefficient α; the discrepancy of the ADC measurement (b) before correction and (c) after correction at five temperatures.

To evaluate the practicality of the correction algorithm, we independently measured the ADC output at five temperatures ranging from −50.0°C to 30.0°C, while providing the same input voltages from 0.2~4.2 V to the circuitry. We

DOI: 10.1587/elex.14.20170876
Received August 23, 2017
Accepted September 11, 2017
Publicized September 28, 2017
Copyedited October 25, 2017

observe that the discrepancy between the ADC measurements and the ideal output given by Eq. (2) at each input voltage and each test temperature, is all within −28.3 counts to 12.4 counts (Fig. 7b). The results also verify the excellent measurement accuracy and repeatability of this ADC circuitry. After correcting these measurements following Eq. (6), we find that the corrected ADC output corresponds well with the ideal output given by Eq. (2), with the discrepancy of −23.4 counts to 10.7 counts over the test temperature range of −50°~30°C (Fig. 7c). Even though the improvement in the discrepancy after the correction process is relatively limited due primarily to the excellent conversion accuracy of the ADC circuitry itself and the slight difference existing in the correction coefficient α at different temperature, the discrepancy after correction still reduces further in general compared with those before correction. This verifies the effectiveness of the correction algorithm developed in this part, which is especially recommended to those ADC measurements where high conversion accuracy is of concern.

6 Performance evaluation of the driver circuitry with the spectrometer

Having examined and corrected the driver circuitry itself, the performance of the driver circuitry together with the spectrometer is examined to verify practicality of the driver circuitry developed in this paper. The working mechanism of the spectrometer determines that signal output of the spectrometer should be proportional to integration time since more photons will be collected and converted into signal output if the integration time is longer. Therefore, the time dependence of the signal output is one of the most straightforward ways to evaluate their performance.

To do this, we put the spectrometer together with the driver circuitry into the environmental chamber and measured the spectrometer output over the same range of −50°~30°C, while providing the spectrometer with a constant light source and varying the integration time via the control of the driver circuitry (Fig. 8). The tungsten light bulb was powered by a stabilized DC power supply to keep this light source as stable as possible. The emitted light was guided to the spectrometer via a fiber and the potential intensity fluctuation was monitored by a photodiode. At each test temperature, we first waited ~20 minutes for their temperature to stabilize before collecting measurements. The measurement was taken 10 times at each of the 10 different integration times ranging from 0.1 s to 8 s, to minimize statistical uncertainty. The primary consideration for adopting such an integration time range was to make the spectrometer output fall into its linear operating range even for the longest integration time (e.g., 8 s), for the light source used in this examination. Meanwhile, the dark output of the spectrometer was also measured at the same integration time settings while there was no light entering the spectrometer, for the subsequent correcting.

We first corrected the influence of the dark output in the spectrometer output by subtraction at each integration time, to get the signal output only. We then averaged the signal output over the measurements collected and corrected the influence of the driver circuitry following Eq. (6). We then normalized the corrected signal output for any intensity fluctuation in the light source as determined by the

DOI: 10.1587/elex.14.20170876
Received August 23, 2017
Accepted September 11, 2017
Publicized September 28, 2017
Copyedited October 25, 2017

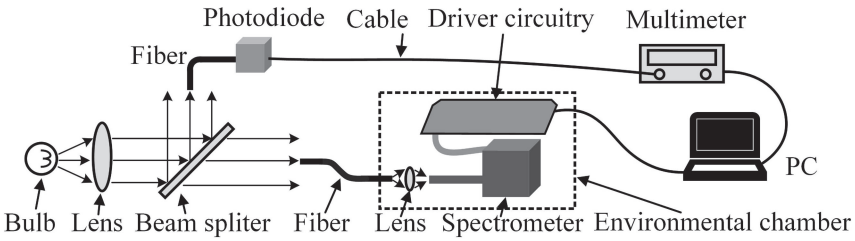

Fig. 8. Test configuration of the driver circuitry with the spectrometer used to assess their performance.

photodiode, by referencing the corresponding photodiode voltage to the one in the first measurement.

The results denote that the general shape of the signal output is very similar for each integration time, but the signal output for each wavelength varies significantly (Fig. 9a). The signal output increases strongly proportionally with longer integration time at each wavelength for all the test temperatures (Fig. 9b), which agrees well with working mechanism of the spectrometer and verifies the practicality of the driver circuitry and the correction algorithm developed in this study. However, signal output decreases significantly with colder temperature for each integration time, this relationship is roughly in a linear manner (Figs. 9c and 9d). When the temperature decreases from 30°C to −50°C, the signal output decreases by ∼36.7% at 533 nm. This temperature-induced biases in the signal output are possibly due to the thermal distortion of the internal optical elements and temperature dependence of the internal electronics of the spectrometer. We notice that the temperature dependence and time dependence of the spectrometer could be modeled and corrected to get the exact spectral intensity of the incident light signal, but it is out of the scope of this study.

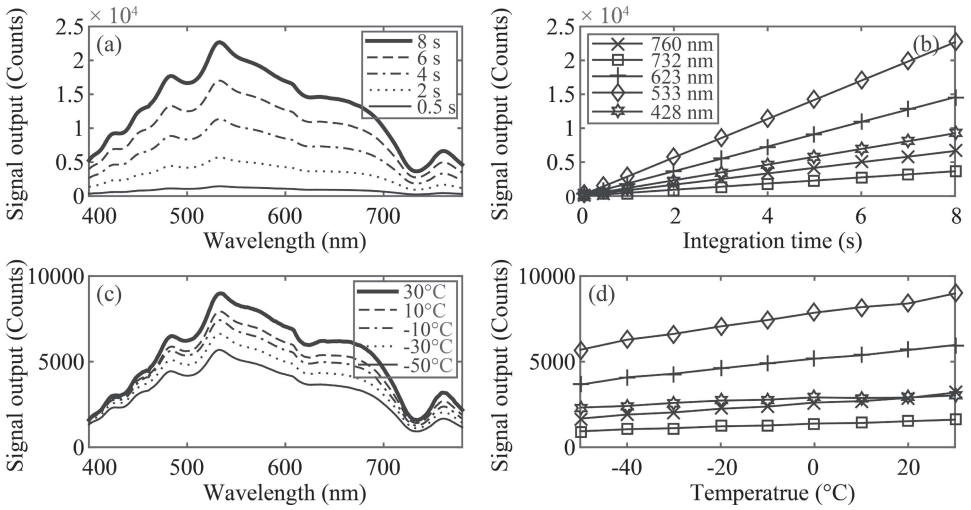

Fig. 9. Signal output as a function of (a) wavelength at five integration times, and (b) integration time at five wavelengths, at −50°C. Signal output as a function of (c) wavelength at five temperatures, and (d) temperature at the same five wavelengths as (b), at 1 s.

DOI: 10.1587/elex.14.20170876
Received August 23, 2017
Accepted September 11, 2017
Publicized September 28, 2017
Copyedited October 25, 2017

7 Conclusion

A driver circuitry for a miniature spectrometer has been developed in this paper, to take charge of the operation of this spectrometer targeting the operating range of −50°∼30°C. Performances of this driver circuitry were evaluated comprehensively over the entire 80°C operating range of temperatures we concerned. And a correction algorithm was developed to correct the biases in the ADC circuitry with an uncertainty of around ±20 Counts. Additionally, even though it had not been discussed in the previous sections, the temperature dependence of the frequency of the TCXO was also examined. It is always stable at 12.8 MHz over −50°∼30°C. These characteristics are good enough for our application. The practicality of this driver circuitry was examined finally, which also testifies the practicality and usefulness of our approach.

Acknowledgments

This work is financially supported by National Natural Science Foundation of China (41606214, 61605038), the National Key Research and Development Program of China (2016YFC1400303), the open foundation of Zhejiang Provincial Top Key Discipline of Mechanical Engineering, and Zhejiang Provincial Postdoctoral Science Foundation funded project.

DOI: 10.1587/elex.14.20170876
Received August 23, 2017
Accepted September 11, 2017
Publicized September 28, 2017
Copyedited October 25, 2017